Blocking effects in flow over obstacles

By ROBERT R. LONG, *Dept. of Mechanics, Johns Hopkins University, Baltimore, Maryland 21213*

(Manuscript received November 11, 1969; revised version April 15, 1970)

ABSTRACT

A theoretical investigation is made of the flow of two fluids over an obstacle. Particular attention is given to the upstream disturbance that occurs when the obstacle is started up from rest in a long channel. This has importance as it relates to the blocking phenomenon that occurs when a stratified fluid like the atmosphere moves over barriers. The results of the analysis are borne out by the experiments in the special case of disturbances at a water-air interface. The blocking that occurs is accomplished by a bore moving up ahead of the obstacle raising the upstream depth. The phenomenon is unsteady; it is also non-linear as indicated by the fact that the upstream may be disturbed even when conditions permit no *infinitesimal* disturbance to progress upstream.

1. Introduction

In papers dealing with problems of air flow over mountains, two assumptions—among others—are commonly made: (1) the mountain is in the form of a ridge, so that the motion may be considered two-dimensional, (2) conditions upstream may be prescribed. These two assumptions are related because in two-dimensional motion, as seen in experiment, the obstacle can drastically affect the approach conditions far upstream whereas this seems unlikely in three-dimensional flows.

One of the earliest papers on this and a related problem was an experimental paper by Taylor (1922) who observed that a sphere moving slowly along the axis of a rotating fluid pushes a column of fluid ahead of it of the same radius as the sphere. More recently, Long (1955) observed strong upstream effects when an obstacle is moved slowly and horizontally in a stratified fluid. In this case, which is more easily observed than the rotating case, the obstacle causes a blocking of the fluid up to the level of the obstacle crest. Above this, there is a high-velocity jet moving toward the obstacle. This, in turn, has another stagnant layer above it and so on, with as many as six or seven sets of alternate jets and stagnation layers for very slow flow and large obstacles. At higher velocities, the picture simplifies. Fig. 1 for example, shows only two blocked regions, one up to the level of the obstacle crest and one just below the free surface. There is a high-velocity region in-between.

Theoretical investigations (Long, 1959; Martin & Long, 1968) have been made of this phenomenon at such low velocities that there is a balance of buoyancy, pressure and viscous forces. Janowitz (1968) conducted a more general investigation including inertial effects by using the Oseen approximation. In all cases, the general flow pattern described above appears upstream and over the obstacle. A simple qualitative explanation for the alternate jets and stagnation layers is fundamental. Thus below the level of the obstacle crest the fluid may be advanced in which the effect of frictionis blocked upstream because of the stratification. With viscosity, this effect weakens upstream so that the approach flow is greater in this layer far from the obstacle than it is closer to the obstacle. This yields a positive vertical velocity as in Fig. 2 and, considering the relative orientation of the constant density and constant pressure surfaces, a generation of vorticity in the sense shown. This yields the vorticity for the lower half of the jet that appears just above the level of the obstacle crest. This jet is strongest near the obstacle because the whole pattern must weaken through viscous action as we look upstream. The result is a downward vertical velocity just above the jet and a generation of vorticity of the opposite sense to support the shear in the upper half of the jet-layer. Continuing up-

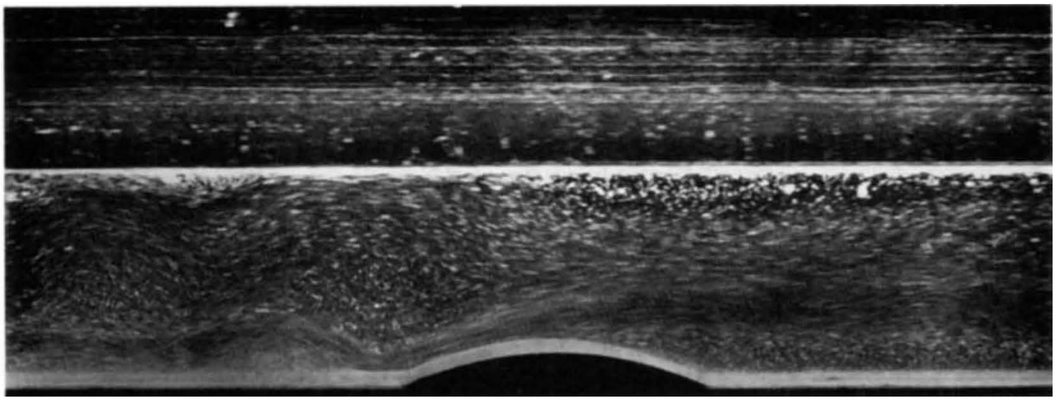

Fig. 1. Pattern of flow of a stratified fluid over an obstacle. In this experiment, the continuous, approximately linear density gradient in the basic state has been obtained by a mixture of salt and water. The tracer is aluminum powder.

ward, we see that from a vorticity viewpoint a whole system of alternate jets and stagnation layers are possible. That viscosity is an essential ingredient in the explanation of the system is also indicated by a theoretical investigation of Bretherton (1967). When he neglected viscosity altogether, he got blocking only at the level of the obstacle. When he allowed a small amount of friction, the alternate jet system tended to appear.

Thus, theoretical and experimental evidence is conclusive that blocking in stratified fluids occurs at low velocities and is of the form indicated above. When the velocity becomes larger but still smaller than the velocity at which all waves are washed downstream, the situation is less clear-cut. The theory of Trustrum (1964) is important in this respect. Using the Oseen approximation, she solved the initial-value problem of stratified-fluid flow in the presence of a disturbance switched on at $t = 0$ at the origin. In most cases, she found disturbances propagating indefinitely far upstream and modifying the upstream velocity distribution. In short, except at the very highest supercritical speeds, it may well be incorrect to prescribe upstream conditions in

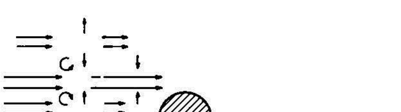

Fig. 2. Schematic picture of blocking motion in flow of a continuously stratified fluid over an obstacle.

constructing mountain-wave solutions, although the mathematical procedure in which these conditions are given is a well-defined and determined one even for finite-amplitude disturbances (Miles, 1969).

An immediate need would seem to be to solve the problem as an initial-value problem, and Trustrum's contribution is a valuable one. But there are uncertainties in her analysis stemming from the Oseen approximation. Indeed, in her solution the disturbance velocities are not small compared to the basic velocity. In addition, one form of blocking in a fluid system involves basic non-linearity in that finite-amplitude wave propagation is a fundamental feature. This is in the flow of a single-fluid or multiple-fluid system over an obstacle in a channel. It has been observed (Long, 1954) that finite-amplitude disturbances frequently form ahead of the barrier and propagate upstream, changing the upstream velocity and density profile. In some cases this occurs at high values of the Froude number in a regime of flow in which linear disturbances cannot move upstream at all. In particular on a water-air interface, this blocking can occur when the original upstream flow yields a Froude number greater than one. The reason, of course, is that non-linear, finite-amplitude disturbances can travel at supercritical speeds and so can penetrate upstream.

In this paper, we investigate theoretically the non-linear, unsteady phenomenon of blocking waves in a two-fluid system and, as a special case of this, at a water-air interface. An experiment is also described in which good agreement with the theory is obtained with regard to disturbances on a water surface.[1]

2. Flow of two fluids over an obstacle

Consider the case of two superimposed fluids moving over a barrier in a channel. For simplicity, we suppose the fluids are contained between two rigid planes at $z = 0$ and $z = H$. The flow with respect to the obstacle is shown in Fig. 3. We have assumed, in accordance with observations in a single fluid system (Long, 1954), that the upstream disturbance is in the form of a wave of elevation or depression moving upstream at speed c relative to the obstacle. In Fig. 4 we have chosen a coordinate system fixed with respect to the wave. Velocities in the coordinate systems are connected by the equations

$$
\begin{aligned}
u_{1a} &= u + c \qquad u_{1b} = u_1 + c = u_{1a}\frac{h_{00}}{h_0} \\
u_{2a} &= u + c \qquad u_{2b} = u_2 + c = u_{2a}\frac{H - h_{00}}{H - h_0}
\end{aligned}
\tag{1}
$$

Momentum considerations. We may derive an equation governing momentum transfer through the entire depth of the fluid on either side of the wave in Fig. 4. This, together with a critical condition at the obstacle crest (see below) and the Bernoulli Equation are insufficient, however, to determine all quantities. We overcome this

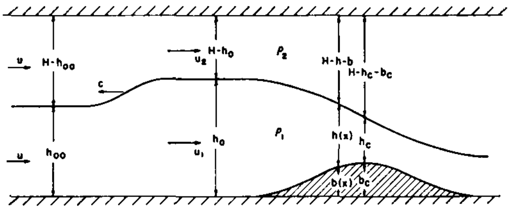

Fig. 3. Flow of two fluids over an obstacle.

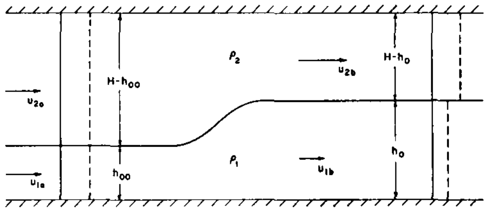

Fig. 4. Flow of two fluids relative to a coordinate system moving with upstream wave disturbance.

problem by deriving momentum equations for both layers of fluid ignoring the momentum exchange across the interface by viscous stresses from the velocity shear at the interface or by turbulent mixing when the wave has the character of a hydraulic jump. It seems likely that this will be a reasonably good approximation for nearly laminar waves. The two momentum equations may be found from Fig. 4. Assuming a pressure $\pi(x)$ on the upper rigid surface, we get for a time interval Δt,

$$
\begin{aligned}
&\frac{1}{\Delta t}[\varrho_2 u_{2b}(u_{2b}\,\Delta t)\,(H-h_0) - \varrho_2 u_{2a}\,(u_{2a}\,\Delta t)\,(H-h_{00})] \\
&\quad = \int_{h_{00}}^{H}[-\varrho_2 g(y-H)+\pi_a]\,dy \\
&\qquad - \int_{h_0}^{H}[-\varrho_2 g(y-H)+\pi_b]\,dy - \int_{\vartheta} p\,dy_s
\end{aligned}
\tag{2}
$$

$$
\begin{aligned}
&\frac{1}{\Delta t}[\varrho_1 u_{1b}(u_{1b}\,\Delta t)\,h_0 - \varrho_1 u_{1a}(u_{1a}\,\Delta t)\,h_{00}] \\
&\quad = \int_0^{h_{00}}[-\varrho_1 g(y-h_{00}) - \varrho_2 g(h_{00}-H)+\pi_a]\,dy \\
&\qquad - \int_0^{h_0}[-\varrho_1 g(y-h_0) - \varrho_2 g(h_0-H)+\pi_b]\,dy \\
&\qquad + \int_{\vartheta} p\,dy_s
\end{aligned}
\tag{3}
$$

where the last integral in each equation is over the interface, $y = y_s(x)$. If we assume hydrostatics in the wave, we have

$$
\int_{\vartheta} p\,dy_s = \int_{\vartheta}[\pi(x) - \varrho_2 g(y_s - H)]\,dy_s \tag{4}
$$

If we now assume[2] a mean value for $\pi(x)$, i.e. $\pi(x) = (\pi_a + \pi_b)/2$, we get

[1] Yih (1969) has given a qualitative discussion of the disturbances that arise when an obstacle is inserted in a stream of water.

[2] This is analogous to the assumption by Yih & Guha (1955) for the case where the upper surface is free. Their theory yielded good agreement with experiment. Yih & Guha also assumed hydrostatics in the wave and a separate momentum condition for each fluid.

$$\int_{\vartheta} p\,dy_s = \frac{(\pi_a+\pi_b)}{2}(h_0-h_{00}) - \varrho_2 g\left[\frac{h_0^2}{2} - Hh_0 - \frac{h_{00}^2}{2} + Hh_{00}\right] \quad (5)$$

The momentum equations become

$$\varrho_2 u_{2b}^2(H-h_0) - \varrho_2 u_{2a}^2(H-h_{00}) = (\pi_a-\pi_b)\left(H-\frac{h_{00}}{2}-\frac{h_0}{2}\right) \quad (6)$$

$$\varrho_1 u_{1b}^2 h_0 - \varrho_1 u_{1a}^2 h_{00} = (\pi_a-\pi_b)\left(\frac{h_0}{2}+\frac{h_{00}}{2}\right) + (\varrho_1-\varrho_2)\frac{g}{2}(h_{00}^2-h_0^2) \quad (7)$$

Critical condition at obstacle crest. The two Bernoulli Equations linking conditions over the obstacle to conditions just upstream are

$$\pi + \frac{\varrho_2 u_2^2(H-h_0)^2}{2(H-h-b)^2} + \varrho_2 gH = \text{const.} \quad (8)$$

$$\pi + \varrho_2 g(H-h-b) + \frac{\varrho_1 u_1^2 h_0^2}{2h^2} + \varrho_1 g(h+b) = \text{const.} \quad (9)$$

Subtracting and evaluating the constant, we get

$$\frac{\varrho_2 u_2^2}{2}\frac{(H-h_0)^2}{(H-h-b)^2} - \frac{\varrho_1 u_1^2}{2}\frac{h_0^2}{h^2} - (\varrho_1-\varrho_2)g(h+b) = \frac{\varrho_2 u_2^2}{2} - \frac{\varrho_1 u_1^2}{2} - (\varrho_1-\varrho_2)gh_0 \quad (10)$$

We now differentiate (10) with respect to x. We get

$$h'\left[\frac{\varrho_2 u_2^2(H-h_0)^2}{(H-h-b)^3} + \frac{\varrho_1 u_1^2 h_0^2}{h^3} - (\varrho_1-\varrho_2)g\right] = b'\left[-\frac{\varrho_2 u_2^2(H-h_0)^2}{(H-h-b)^3} + (\varrho_1-\varrho_2)g\right] \quad (11)$$

where primes denote derivatives. Thus at the crest of the barrier where $b'=0$, we must have $h'=0$, or

$$N = \frac{\varrho_2 u_2^2(H-h_0)^2}{(H-h_c-b_c)^3} + \frac{\varrho_1 u_1^2 h_0^2}{h_c^3} - (\varrho_1-\varrho_2)g = 0 \quad (12)$$

We refer to this as the critical condition at the crest and, in accordance with observations of a single-fluid system (Long, 1954), assume that it is associated with the occurrence of a wave upstream. If $N>0$, we say that conditions are supercritical. If $N<0$, we say that conditions are subcritical. These reduce to standard definitions in the case of a single fluid.

Bernoulli Equation. Finally, Eq. (10) applied at the crest is

$$\frac{\varrho_2 u_2^2}{2}\left[\frac{(H-h_0)^2}{(H-h_c-b_c)^2}-1\right] - \frac{\varrho_1 u_1^2}{2}\left[\frac{h_0^2}{h_c^2}-1\right] = (\varrho_1-\varrho_2)g(h_c+b_c-h_0) \quad (13)$$

We now use (1) to refer Eqs. (6), (7), (12) and (13) to conditions far upstream. We get

$$\frac{\varrho_2(u+c)^2\left[\dfrac{(H-h_{00})^2}{(H-h_0)} - (H-h_{00})\right]}{\left(H-\dfrac{h_{00}}{2}-\dfrac{h_0}{2}\right)} = \frac{\varrho_1(u+c)^2\left[\dfrac{h_{00}^2}{h_0} - h_{00}\right] - (\varrho_1-\varrho_2)\dfrac{g}{2}(h_{00}^2-h_0^2)}{\left(\dfrac{h_0}{2}+\dfrac{h_{00}}{2}\right)} \quad (14)$$

$$\varrho_2\left[(u+c)\frac{(H-h_{00})}{(H-h_0)} - c\right]^2 \frac{(H-h_0)^2}{(H-h_c-b_c)^3} + \varrho_1\left[(u+c)\frac{h_{00}}{h_0} - c\right]^2\frac{h_0^2}{h_c^3} = (\varrho_1-\varrho_2)g \quad (15)$$

$$\frac{\varrho_2}{2}\left[(u+c)\frac{(H-h_{00})}{(H-h_0)} - c\right]^2\left[\frac{(H-h_0)^2}{(H-h_c-b_c)^2}-1\right] - \frac{\varrho_1}{2}\left[(u+c)\frac{h_{00}}{h_0}-c\right]^2\left[\frac{h_0^2}{h_c^2}-1\right] = (\varrho_1-\varrho_2)g(h_c+b_c-h_0) \quad (16)$$

Notice that these equations reduce to those for a single fluid if we put[1] $\varrho_2=0$ *or* if we let $H\to\infty$. In the latter case g is replaced by "reduced gravity", $g'=g(\varrho_1-\varrho_2)/\varrho_1$. Thus we have the well-known result that a two-fluid system consisting of a very deep upper fluid behaves as a single-fluid system in a reduced gravity field.

[1] We give a special discussion of this case in the next section.

Let us now non-dimensionalize with the following definitions:

$$F^2=\frac{u^2}{g'h_{00}},\ \Gamma^2=\frac{c^2}{g'h_{00}},\ R=\frac{h_0}{h_{00}},\ R_c=\frac{h_c}{h_{00}},$$
$$B_c=\frac{b_c}{h_{00}},\ r=\frac{H}{h_{00}} \tag{17}$$

We also make the Boussinesq approximation in which we ignore differences in ϱ_1 and ϱ_2 except in the gravity terms of the equations. Eqs. (14)–(16) become

$$(F+\Gamma)^2\left[\left(\frac{(r-1)^2}{r-R}-(r-1)\right)\frac{R+1}{2}-\left(\frac{1}{R}-1\right)\right.$$
$$\left.\times\left(r-\frac{1}{2}-\frac{R}{2}\right)\right]=-\frac{1}{2}(1-R^2)\left(r-\frac{1}{2}-\frac{R}{2}\right) \tag{18}$$

$$\left[(F+\Gamma)\frac{(r-1)}{(r-R)}-\Gamma\right]^2\frac{(r-R)^2}{(r-R_c-B_c)^3}$$
$$+\left[\frac{(F+\Gamma)}{R}-\Gamma\right]^2\frac{R^2}{R_c^3}=1 \tag{19}$$

$$\frac{1}{2}\left[(F+\Gamma)\frac{(r-1)}{(r-R)}-\Gamma\right]^2\left[\frac{(r-R)^2}{(r-R_c-B_c)^2}-1\right]$$
$$-\frac{1}{2}\left[\frac{(F+\Gamma)}{R}-\Gamma\right]^2\left[\frac{R^2}{R_c^2}-1\right]=R_c+B_c-R \tag{20}$$

Energy considerations. These equations may be solved for the unknowns Γ, R, R_c although we do not present results in this paper in the general case. In solving them, however, we must insure that there is no energy *increase* through the bore. We do this as follows: the energy equation for the fluid in any volume V with boundary B is

$$-\varepsilon^2=\frac{d}{dt}\iiint_V\left(\frac{\varrho q^2}{2}+\varrho g y\right)dV+\iint_B v_n p\,da \tag{21}$$

where ε^2 is positive and the time differentiation is following the fluid which occupies the volume at time t. The quantity v_n is the outward normal velocity at the boundary. If we apply (21) to the fluid originally between the two vertical solid lines in Fig. 4 we get

$$\varrho_2\frac{u_{2b}^3}{2}(H-h_0)+\varrho_1\frac{u_{1b}^3}{2}h_0-\varrho_2\frac{u_{2a}^3}{2}(H-h_{00})$$
$$-\varrho_1\frac{u_{1a}^3}{2}h_{00}+(\pi_b-\pi_a)\left[u_{2a}(H-h_{00})+u_{1a}h_{00}\right]$$
$$+(\varrho_1-\varrho_2)gu_{1a}h_{00}(h_0-h_{00})=-\varepsilon^2 \tag{22}$$

Using Eq. (1) and the sum of Eqs. (6) and (7), this may be written

$$\frac{(u+c^2)}{g'}\left[\frac{h_{00}}{h_0^2}+\frac{\varrho_2}{\varrho_1}\frac{H-h_{00}}{(H-h_0)^2}\right]-1$$
$$=-\frac{2\varepsilon^2}{(u+c)(h_{00}-h_0)^2g'} \tag{23}$$

Using (14) in the form

$$\frac{(u+c)^2}{g'}\left[\frac{2\varrho_2}{\varrho_1}\frac{(H-h_{00})}{(H-h_0)(2H-h_{00}-h_0)}\right.$$
$$\left.+\frac{2h_{00}}{h_0(h_0+h_{00})}\right]=1 \tag{24}$$

We get

$$\frac{\dfrac{h_{00}}{h_0^2}+\dfrac{\varrho_2}{\varrho_1}\dfrac{H-h_{00}}{(H-h_0)^2}}{\dfrac{2h_{00}}{h_0(h_0+h_{00})}+\dfrac{2\varrho_2}{\varrho_1}\dfrac{(H-h_{00})}{(H-h_0)(2H-h_{00}-h_0)}}-1$$
$$=-\frac{2\varepsilon^2}{(u+c)(h_{00}-h_0)^2g'} \tag{25}$$

Since the denominator in the first term of (25) is always positive, we may write

$$(h_{00}-h_0)\left[\frac{h_{00}}{h_0^2(h_0+h_{00})}\right.$$
$$\left.-\frac{\varrho_2}{\varrho_1}\frac{(H-h_{00})}{(H-h_0)^2(2H-h_{00}-h_0)}\right]<0 \tag{26}$$

or, if $s=\varrho_2/\varrho_1$,

$$A\equiv(1-R)\left[\frac{1}{R^2(1+R)}-\frac{s(r-1)}{(r-R)^2(2r-1-R)}\right]<0 \tag{27}$$

We investigate this condition by setting $R=1+\varepsilon$, where ε is small. Then, approximately,

$$A=-\frac{\varepsilon}{2}\left[1-\frac{s}{(r-1)^2}-\frac{5}{2}\varepsilon-\frac{5}{2}\varepsilon\frac{s}{(r-1)^3}\right] \tag{28}$$

Thus if $s=(r-1)^2$, then to this order, $A>0$ and so no disturbance of the type foreseen in this analysis can propagate upstream. In the case of interest here, when $s = 1$ (Boussinesq approximation), (27) yields an energy loss for a hydraulic jump when $r > 2$ and for a hydraulic drop when $r < 2$, i.e. when the depth of the lower fluid is less than or greater than that of the upper fluid. When $s = 0$, the results reduce to those for a single fluid, namely $R > 1$.

3. Single-fluid system

The equations of the two-fluid case are complicated algebraically, and it is simplest to confine attention here to a theoretical and experimental study of the case of a single fluid. The equations corresponding to (18)–(20) may be obtained by putting $\varrho_2 = 0$ in Eqs. (14)–(16). Then, in terms of the quantities in Eq. (17), (except with F replaced by the ordinary Froude number) we get

$$2(F+\Gamma)^2\left(\frac{1}{R}-1\right)=(1-R^2) \tag{29}$$

$$\frac{R^2}{R_c^3}\left[\frac{F+\Gamma}{R}-\Gamma\right]^2=1 \tag{30}$$

$$\frac{1}{2}\left[\frac{F+\Gamma}{R}-\Gamma\right]\left[\frac{R^2}{R_c^2}-1\right]=R-R_c-B_c \tag{31}$$

In these equations, B_c and F are given and Γ, R and R_c are to be determined. We do this as follows: we write Eqs. (29)–(31) as

$$\Gamma=-F+\left[\frac{R(1+R)}{2}\right]^{\frac{1}{2}} \tag{32}$$

$$R_c=[F-\Gamma(R-1)]^{\frac{2}{3}} \tag{33}$$

$$B_c=R-\frac{3}{2}R_c+\frac{1}{2}\frac{R_c^3}{R^2} \tag{34}$$

We fix F and R. Then Eq. (32) determines Γ, Eq. (33) determines R_c and Eq. (34) determines B_c. As the computation proceeds, R_c may fall to zero. For higher values of B_c the fluid is unable to move over the obstacle. In the plane of R and B_c this corresponds to the straight line $B_c = R$. On the other hand, Γ may be negative. We reject this solution since it corresponds to a blocking wave moving *toward* the barrier. The curve corresponding to $\Gamma = 0$ is

$$B_c=R+\frac{1}{4R}+\frac{1}{4}-\frac{3}{2}\left[\frac{R(1+R)}{2}\right]^{\frac{1}{3}} \tag{35}$$

Finally, we reject all solutions corresponding to $R < 1$. The computed results are shown in Figs. 5–7.

The experimental measurements related to this theory were performed in a long channel containing water of depth h_{00} using a long obstacle. The obstacle is started up from rest in the channel and moved at constant speed for some time. The obstacle is drawn down the channel by a thin line wrapped around a cylindrical winder. The winder is driven by a variable-speed transmission and motor. To find u, or the velocity with which the obstacle moves down the channel, it is only necessary to know the rpm of the winder and its circumference. The velocity is then computed by counting a large number of revolutions.

The obstacles were formed from thick sheets of plexiglas folded over crossribs cut to the desired obstacle shape. Two obstacles were used, one 9.1 cm high and the other 2.0 cm high in a channel 15 cm wide.

Leakage between the obstacle and the sides of the channel was a problem. The tendency, of course, is to lower the R-values when blocking occurs ahead of the obstacle. The leaking was reduced by widening the obstacle with thin sheets of plexiglas until the barrier could just barely pass down the channel. Leakage under the obstacle also occurred, but was minimized by weighing the obstacle down. The difficulty here was greatest at high speeds as the obstacle tended to lift off the bottom.

Greater experimental difficulties arose in creating flows at the higher Froude numbers. As the speed of the obstacle increased, the time available to measure depths ahead of it was reduced. On the other hand, because variation in the denominator of F is as the square root of the depth, reducing the depth to increase F was not very effective. In addition the use of shallower depths increased the percentage error in the depth measurements. A combination of the above two methods was finally employed. By using an obstacle 2 cm high moving at a velocity of $1\frac{1}{2}$ feet per second, a Froude number of approximately one was achieved for a ratio of $B_c = 1$.

There were other difficulties at the higher Froude numbers. For example, the difference between the speed of the jump and the speed of

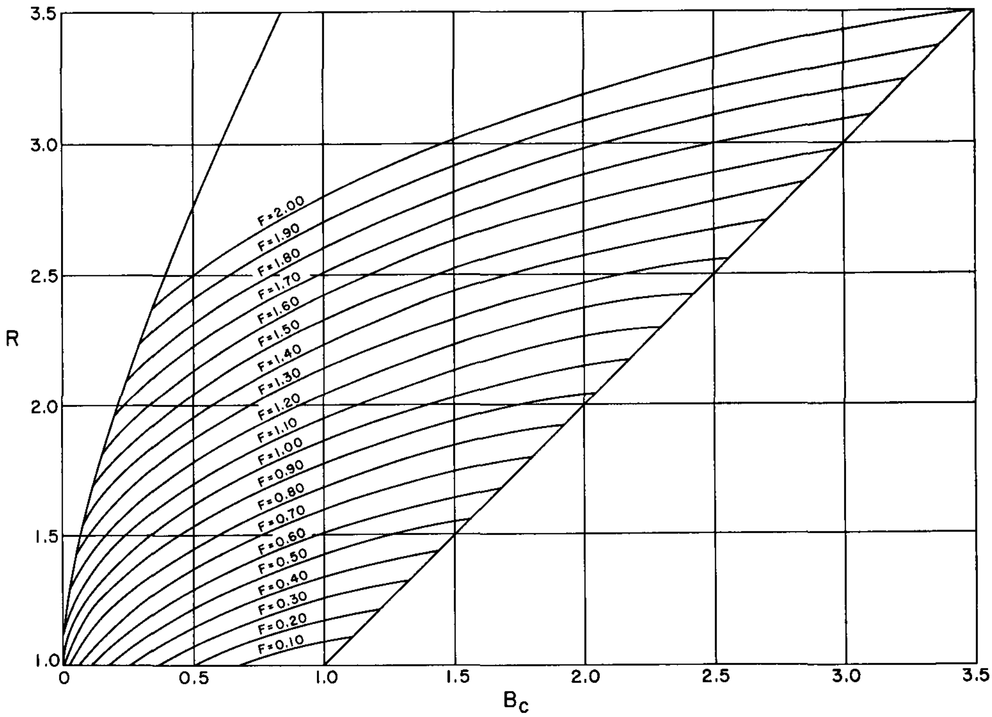

Fig. 5. Solution of Eqs. (32)–(34) for R as a function of B_c and F.

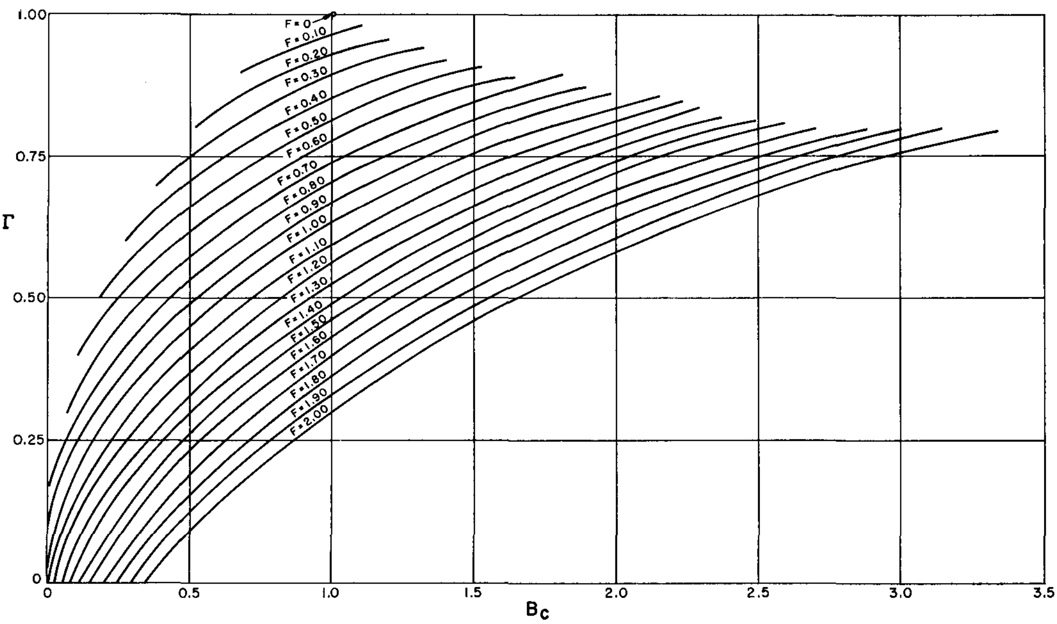

Fig. 6. Solution of Eqs. (32)–(34) for Γ as a function of B_c and F.

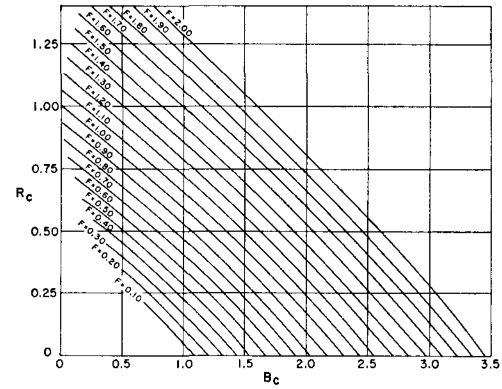

Fig. 7. Solution of Eqs. (32–(34) for R_c as a function of B_c and F.

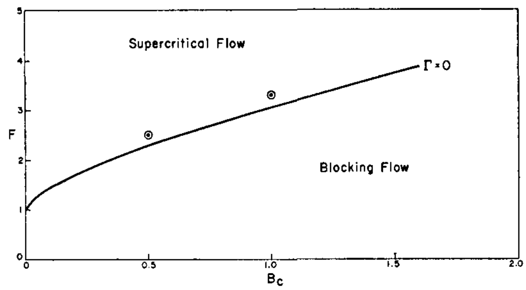

Fig. 9. Observations at Froude numbers above the curve $\Gamma = 0$ in the supercritical region.

the obstacle becomes so small as $\Gamma \to 0$ that there is very little space between the obstacle and jump in which to measure depths. Furthermore, the fluid immediately ahead of the obstacle becomes involved in the turbulence behind the jump so that the level h_0 and hence R fluctuates to make measurements uncertain.

Finally, some difficulty of measurement results from the curvature of the free surface against the glass sides of the channel due to surface tension. This, together with the parallax misalignment of the observer's eye and the scale through the thick glass walls, added further error.

Six quantities were measured in the experiment: obstacle height b_c, water depth at rest h_{00}, the obstacle speed u, the level of water just ahead of the obstacle h_0, the speed of the moving upstream jump c, and the water depth above the crest of the obstacle h_c. The non-dimensional quantities in the graphs in Figs. 5–7 may be calculated using these six quantities. The measuring equipment consisted of a metric scale graduating in millimeters and a standard stop watch. It is estimated that depth measurements are accurate to 0.5 mm and time measurements to 0.1 sec.

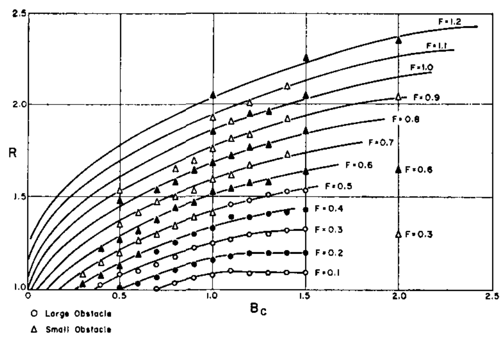

Fig. 8. Experimental measurement of R, B_c and F. The theoretical curves are those in Fig. 5. The circles and triangles refer to the large obstacle and the small obstacle, respectively.

The channel sloped about 2 mm/meter in the direction of motion of the obstacle. Since the water surface is initially level, h_{00} varies when measured at different stations by as much as 4 mm over the 2 meter-long path of the obstacle. Since h_{00} is used to calculate B_c, F, R, R_c and Γ, a corresponding error is introduced in all these values as well. This was minimized by using an average depth h_{00} over the path of the obstacle and by measuring all other depths relative to the level of the resting water surface. This error tended to lower the measured R-values but some compensation was provided by a small parallax error of about 0.5 mm in reading the water level ahead of the obstacle and by an error due to the surface tension lip at the side of the channel.

The most accurate of the measured quantities is the Froude number since the obstacle speed can be measured very accurately as noted above. Some of the experimental results are shown in Fig. 8 in which data is entered on the theoretical curves of Fig. 5. The agreement is generally good but, as explained above, the data becomes less accurate and more difficult to obtain at the higher Froude numbers. Indeed, no attempt was made to obtain measurements when the jump spread was low (Γ near zero). We did verify the $\Gamma = 0$ curve, however, in that supercritical flow was observed above this line. Two cases are shown in Fig. 9.

Fig. 10 taken from Fig. 7 shows measurements

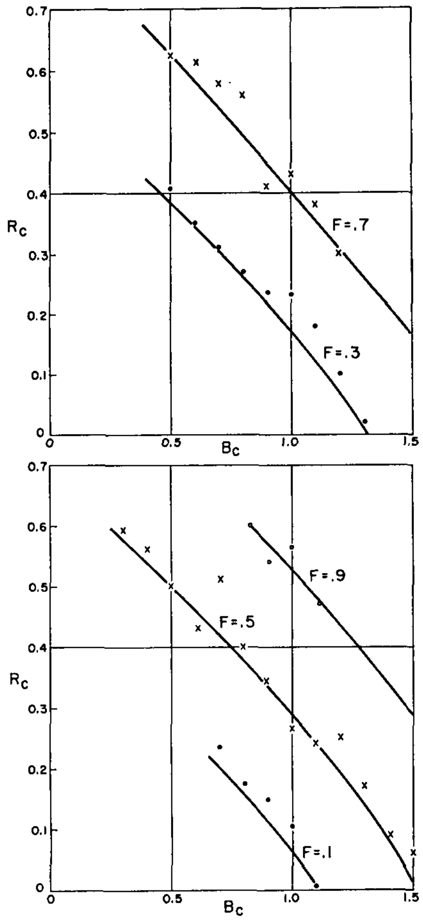

Fig. 10. Experimental measurements of R_c, F and B_c. The theoretical curves are those of Fig. 7.

of R_c. The agreement is rather poor since, as we have noted, it was very difficult to get accurate measurements of h_c. This was especially true at the higher Froude numbers and velocities. The main tendency was to read the depth h_0 ahead of the obstacle rather that the smaller depth h_c. This resulted in h_c values being too large in most cases as shown by the data. Only in regions of deep water were the measurements in reasonably good agreement with calculations.

By way of contrast, there is no single direction of the error in the measured values of Γ as we see in Fig. 11 taken from Fig. 6 of the theory. One source of error in measuring wave speeds comes from the ± 0.1 sec error in the stop-watch readings since there was no way to increase the measuring times. A measured length of $6\frac{1}{2}$ ft was used, and an average absolute time for the wave to travel this distance might be 2.6 ± 0.1 sec corresponding to a 4% error. This yields an average velocity of 2.5 ± 0.1 ft/sec. Subtracting the accurately determined obstacle speed from this to give the relative velocity between the jump and the obstacle lowers the magnitude of the relative velocity to about 1 ft/sec on the average, and the error is now about 10%. Most of the measured values of Γ were within a 10% error of the calculated values, and in most cases the error was not in any one preferred direction. An additional source of error in measuring speed of the jump occurs at the lower Froude numbers.

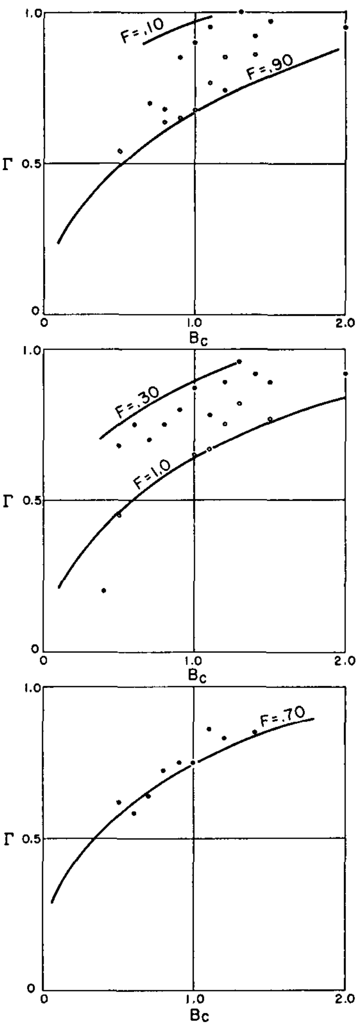

Fig. 11. Experimental measurements of Γ, F, and B_c. The theoretical curves are those of Fig. 6.

When F is in the range 0.0–0.3 the upstream disturbance is in the form of an undular hydraulic jump which appears as a series of long, low waves. Finding a fixed point in the first wave was a recurring problem. Furthermore, the situation may not have been steady in that the succeeding waves traveling behind the first one may not have been moving at the same speed.

In the regime of totally blocked flows, the measured values of R in Fig. 8 remain constant with B_c, since the precise height of the obstacle is of no importance once total blocking occurs. The measured value was generally slightly less than the value of F at which the corresponding Froude-number curve in Fig. 5 crosses the line $R = B_c$. This discrepancy was probably due to the increased importance of leakage at the low depths corresponding to large values of B_c. The upstream jump in the totally-blocked case is the same as the partially-blocked case at the same Froude number.

Mention may be made of the transition to subcritical flow. The subcritical region begins at the predicted value of F and B_c. Transition from the blocked flow to the subcritical flow occurs as the upstream wave disturbance becomes smaller and smaller and finally can no longer be detected.

Acknowledgement

This research was supported by the Environmental Science Services Administration under Grant No. E22-15-69(G).

REFERENCES

Bretherton, F. P. 1967. The time-dependent motion due to a cylinder moving in an unbounded rotating or stratified fluid. *J. Fluid Mech. 28*, 545.

Janowitz, G. S. 1968. On wakes in stratified fluids. *J. Fluid Mech 33*, 417.

Long, R. R. 1954. Some aspects of the flow of stratified fluids. II. Experiments with a two-fluid system. *Tellus 6*, 97.

Long, R. R. 1955. Some aspects of the flow of stratified fluids. III. Continuous density gradients. *Tellus 7*, 341.

Long, R. R. 1959. The motion of fluids with density stratification. *J. Geophys. Res. 64*, 2151.

Martin, S. & Long, R. R. 1968. The slow motion of a flat plate in a viscous, stratified fluid. *J. Fluid Mech. 31*, 669.

Miles, J. W. 1969. A slender body in a rotating flow. *J. Fluid Mech. 36*, 265.

Taylor, G. I. 1922. The motion of a sphere in a rotating liquid. *Proc. Roy. Soc. (A) 102*, 180.

Trustrum, K. 1964. Rotating and stratified fluid flow. *J. Fluid Mech. 19*, 415.

Yih, C. S. & Guha, C. R. 1955. Hydraulic jump in a fluid system of two layers. *Tellus 8*, 358.

Yih, C. S. 1969. Stratified flows. *Annual Reviews in Fluid Mechanics*, pp. 98–100

ЭФФЕКТ БЛОКИРОВАНИЯ В ПОТОКЕ НАД ПРЕПЯТСТВИЕМ

Проделано теоретическое исследование потока двуслойной жидкости над препятствием. Особое внимание обращено на распространение возмущений вверх по течению, когда препятствие начинает двигаться из состояния покоя в длинном канале. Этот важный вопрос связан с блокированием, которое имеет место, когда стратифицированная жидкость, подобная атмосфере, движется над препятствиями. Результаты анализа подтверждаются экспериментами в специальном случае возмущений на поверхности раздела вода–воздух. Блокирование создается борой, движущейся впереди препятствия и увеличивающей глубину вверх по течению. Явление нестационарно; оно также нелинейно. Последнее подтверждается тем фактом, что поток вверх по течению может быть возмущен, даже когда условия не допускают распространения бесконечно малых возмущений вверх по течению.